Ferromagnetism in Mn-implanted ZnO:Sn single crystals

D. P. Norton[a] and S. J. Pearton
Department of Materials Science and Engineering, University of Florida, 106 Rhines Hall, P.O. Box 116400, Rhines Hall, Gainesville, Florida 32611

A. F. Hebard and N. Theodoropoulou
Department of Physics, University of Florida, Gainesville, Florida 32611-8440

L. A. Boatner
Solid State Division, Oak Ridge National Laboratory, Oak Ridge, Tennessee 37831

R. G. Wilson
Consultant, Stevenson Ranch, California 95131

(Received 30 July 2002; accepted 21 November 2002)

We have investigated the magnetic properties of Mn-implanted *n*-type ZnO single crystals that are codoped with Sn. Theory predicts that room-temperature carrier-mediated ferromagnetism should be possible in manganese-doped *p*-type ZnO, although Mn-doped *n*-type ZnO should not be ferromagnetic. While previous efforts report only low-temperature ferromagnetism in Mn-doped ZnO that is *n* type via shallow donors, we find evidence for ferromagnetism with a Curie temperature of ~250 K in ZnO that is codoped with Mn and Sn. As a 4+ valence cation, Sn should behave as a doubly ionized donor, thus introducing states deep in the gap. Hysteresis is clearly observed in magnetization versus field curves. Differences in zero-field-cooled and field-cooled magnetization persists up to ~250 K for Sn-doped ZnO crystals implanted with 3 at.% Mn. Increasing the Mn concentration to 5 at.% significantly reduces the magnetic hysteresis. This latter observation is inconsistent with the origin for ferromagnetism being due to segregated secondary phases, and strongly suggests that a near-room-temperature dilute magnetic semiconducting oxide has been realized. Based on these results, ZnO doped with Mn and Sn may prove promising as a ferromagnetic semiconductor for spintronics. © *2003 American Institute of Physics.*
[DOI: 10.1063/1.1537457]

In recent years, ferromagnetism in semiconductors has received significant attention, partly due to interest in spintronic device concepts.[1–5] Much of the recent effort has focused on conventional II–VI and III–V semiconductor materials. Low-temperature epitaxial growth has been used with Mn-doped GaAs (Ref. 6) in achieving ferromagnetism with a transition temperature of 110 K, which is remarkably high compared to traditional dilute magnetic semiconductor material. More recently, ferromagnetism has been reported at temperatures above 300 K for $(Cd_{0.95}Mn_{0.05})GeP_2$,[7] $Zn_{1-x}Mn_xGeP_2$,[8,9] GaMnN,[10,11] GaMnP,[12] $Co-TiO_2$,[13,14] and $ZnSnAs_2$.[15]

The origin of ferromagnetism in semiconductors remains an issue of debate.[16] Dietl *et al.* have applied Zener's model for ferromagnetism, driven by exchange interaction between carriers and localized spins, to explain the ferromagnetic transition temperature in III–V and II–VI compound semiconductors. The theory assumes that the ferromagnetic correlations among the Mn ions are mediated by holes from shallow acceptors. Specifically, Mn ions substituted on the group II or III site provide the local spin. In the case of III–V semiconductors, Mn also provides the acceptor dopant. Direct exchange among Mn is antiferromagnetic as observed in fully compensated (Ga, Mn)As that is donor doped. In the case of electron-doped or heavily Mn-doped GaAs material, no ferromagnetism is detected. The model suggests that carrier-mediated ferromagnetism in *n*-type material is relegated to low temperatures, as seen for example in *n*-type GaMnN,[17] while it is predicted at higher temperatures for *p*-type materials.[18] It has been reasonably successful in explaining the high transition temperature observed for (Ga, Mn)As.

The theoretical treatment presents several interesting trends and predictions. For the materials considered in detail (semiconductors with zinc-blende structure), magnetic interactions are favored in hole-doped materials due to the interaction of Mn^{2+} ions with the valence band. This is consistent with previous calculations for the exchange interaction between Mn^{2+} ions in II–VI compounds,[3,19,20] showing that the dominant contribution is from two-hole processes. This superexchange mechanism can be viewed as an indirect exchange interaction mediated by the anions, thus involving the valence band. Note that valence-band properties are primarily determined by anions in II–VI compounds. The model by Dietl *et al.* predicts that the transition temperature will scale with a reduction in the atomic mass of the constituent elements due to an increase in $p-d$ hybridization and a reduction in spin-orbit coupling. Most importantly, the theory predicts a T_c greater than 300 K for *p*-type GaN and ZnO, with T_c dependent on the concentration of magnetic ions and holes. However, it also predicts that ferromagnetism will not be observed at high temperature for electron-doped ZnO, at least for dopants that introduce shallow donor levels.

Magnetically doped ZnO has also been theoretically in-

[a]Author to whom correspondence should be addressed; electronic mail: dnort@mse.ufl.edu

vestigated by *ab initio* calculations based on local density approximation.[21] Again, the results suggest that ferromagnetic ordering of Mn is favored when mediated by hole doping. For V, Cr, Fe, Co, and Ni dopants, ferromagnetic ordering in ZnO is predicted to occur without additional charge carriers. Recently, the magnetic properties of Ni-doped ZnO thin films were reported.[22] For films doped with 3–25 at. % Ni, ferromagnetism was observed at 2 K. Above 30 K, superparamagnetic behavior was observed. The ZnO material was *n* type. Fukumura *et al.* have shown that epitaxial thin films of Mn-doped ZnO can be obtained by pulsed-laser deposition, with Mn substitution as high as 35% while maintaining the wurtzite structure.[23] This is well above the equilibrium solubility limit of ~13%, and illustrates the utility of low-temperature epitaxial growth in achieving metastable solubility in thin films. Codoping with Al resulted in *n*-type material with carrier concentration in excess of 10^{19} cm^{-3}. Large magnetoresistance was observed in the films, but no evidence for ferromagnetism was reported. However, Jung *et al.* recently reported ferromagnetism in Mn-doped ZnO epitaxial films, with a Curie temperature of 45 K.[24] The discrepancy appears to lie in differing film-growth conditions.

In this letter, we report evidence for ferromagnetism in ZnO with a Curie temperature approaching 250 K. For these materials, Mn serves as the transition metal and Sn as an apparent doubly ionized donor dopant. ZnO is a direct-band-gap semiconductor with $E_g = 3.35$ eV. The room-temperature Hall mobility in ZnO single crystals is on the order of 200 $cm^2 V^{-1} s^{-1}$.[25] Electron doping via defects originates from Zn interstitials in the ZnO lattice.[26] The intrinsic defect levels that lead to *n*-type doping lie approximately 0.05 eV below the conduction band. High electron carrier density can also be realized via group III substitutional doping. As a group IV cation, Sn can exist in either the 4+ or 2+ valence state, although the 4+ valence is the most common. As such, it can serve either as a doubly ionized donor or as an isoelectronic impurity.

In the experiments reported here, Mn ions were implanted at elevated temperature into Sn-doped ZnO single crystals. The ZnO substrates were grown via vapor transport. Hall measurements performed prior to implantation yielded a carrier density on the order of 10^{18} cm^{-3}. The Sn-doped ZnO crystals exhibit a blue tint in color and are *n* type. The Sn content was approximately 10^{18} cm^{-3}. Mn^+ ions were implanted at a dose of $\sim 5 \times 10^{16}$ cm^{-2} and energy of 250 keV into the (110) ZnO growth face, with substrates held at 350 °C to avoid amorphization. The projected range of Mn ions was estimated to be 150 nm with the implant designed to yield a Gaussian profile. The targeted peak Mn concentrations investigated in this study were 3 and 5 at. %. Following implantation, the samples were subjected to a 5 min, 700 °C rapid thermal anneal in flowing nitrogen. Figure 1 shows EDS spectra for a Mn-implanted sample. The Mn peak intensity is consistent with a doping concentration of a few atomic percent. Note that no evidence for nitride formation is observed, nor is it expected based on the bonding energy of N_2.

The magnetic properties of Mn-implanted samples were measured using a Quantum Design superconducting quantum interference device magnetometer. Figure 2 shows the

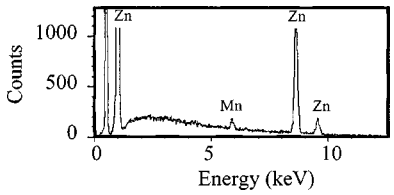

FIG. 1. Energy dispersive spectrometry (EDS) data for a Mn-implanted ZnO single crystal. The EDS intensity for the Mn peak is consistent with a Mn concentration of a few atomic percent.

magnetization versus field behavior at 10 K for Sn-doped ZnO samples implanted with 3 and 5 at. % Mn. Hysteretic behavior is clearly observed, consistent with ferromagnetism. At 10 K, the coercive field in the 3 at. % Mn-doped sample is 250 Oe. It must be noted that other possible explanations for hysteretic *M* vs *H* behavior that are remotely possible include superparamagnetism and spin-glass effects.[6,19,27] Magnetization measurements were also performed on Sn:ZnO crystals that were not subjected to the Mn implant. This was done to eliminate the possibility that spurious transition metal impurities might be responsible for the magnetic response. The Sn-doped ZnO crystals exhibit no hysteresis, showing that the Mn doping is responsible for the behavior. To track the hysteretic behavior in the implanted samples as a function of temperature, both field-cooled and zero-field-cooled magnetization measurements were performed from 4.2 to 300 K. By taking the difference between these two quantities, the para- and diamagnetic contributions to the magnetization can be subtracted, leaving only a measure of the hysteretic ferromagnetic regime. Figure 3 shows the difference between field-cooled and zero-field-cooled magnetization as a function of temperature for both the 3 at. % Mn- and 5 at. % Mn-doped samples. For the 3 at. % Mn sample, in particular, a robust ferromagnetic signature is observed to persist up to ~250 K, as seen in Fig. 4.

When assigning the origin of ferromagnetism one must carefully consider the possibility that secondary phase formation is responsible. High-resolution transmission electron

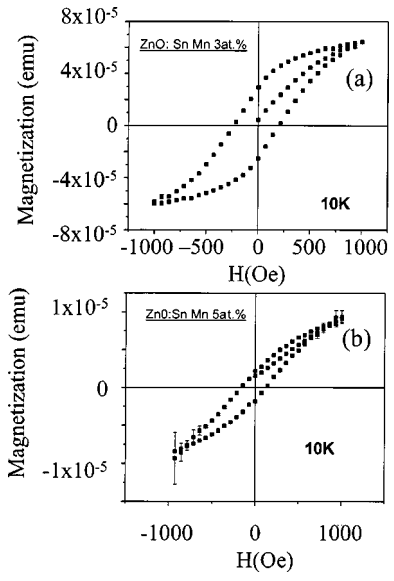

FIG. 2. *M* vs *H* curve for Mn-implanted ZnO:Sn single crystals, showing ferromagnetic behavior in (a) 3 at. % Mn and (b) 5 at. % Mn implantation doses.

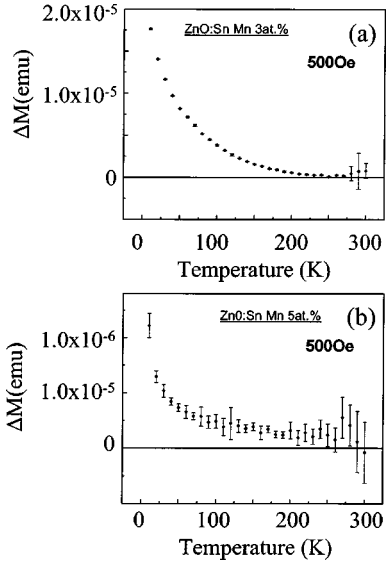

FIG. 3. Temperature dependence of the difference between field-cooled and zero-field-cooled magnetizations for (a) 3 at. % and (b) 5 at. % implanted Mn concentrations in ZnO:Sn crystal. Note that the magnetization is significantly larger for the 3 at. % Mn-doped sample.

microscopy is currently being pursued for the Mn-implanted ZnO samples. Nevertheless, one can also consider what known ferromagnetic impurity phases are possible. First, metallic Mn is antiferromagnetic, with a Néel temperature of 100 K. In addition, nearly all of the possible Mn-based binary and ternary oxide candidates are antiferromagnetic. The exception to this is Mn_3O_4, which is ferromagnetic with a Curie temperature of 42 K. X-ray diffraction measurements show no evidence for Mn–O phases, although diffraction is inadequate to detect secondary phases at the level necessary. However, even if this phase were present, it could not account for the ferromagnetic transition temperature of ~250 K observed for the Mn-implanted ZnO:Sn crystals. Note, also, that the Mn concentrations used in this study were well below the solid solubility limit of Mn in ZnO. It should also be noted that increasing the Mn content from 3 to 5 at. % resulted in a significant decrease in the relative magnetization response as is seen in Fig. 3. This provides strong evidence, albeit indirect, that the magnetization is not due to any precipitating secondary phase. If the formation of a secondary Mn-related phase was responsible for the ferromagnetic behavior, an increase in Mn concentration would presumably increase the secondary phase volume fraction and related magnetization signature. Instead, the opposite behavior is observed.

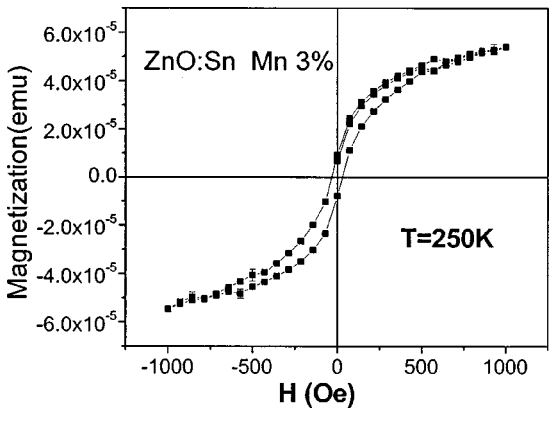

FIG. 4. *M* vs *H* curve at 250 K for the 3 at. % Mn implanted ZnO sample.

One must explain why the behavior depends on the specific cation dopant specie chosen (Sn vs Al, Ga). Doping via a multi-ionized impurity introduces relatively deep donor levels in the energy gap. Conduction from deep donors is due to impurity band and/or hopping conduction, as opposed to conventional free electrons excited to the conduction band. Any carrier-mediated processes would be dependent on the relevant conduction mechanisms. Future work will focus on understanding the effect of carrier density and transition metal concentration on magnetization behavior.

Support for this work was provided by the National Science Foundation under Grant Nos. DMR-9705224 and DMR-0101856.

[1] S. A. Wolf, J. Supercond. **13**, 195 (2000).
[2] G. A. Prinz, Science **282**, 1660 (1998).
[3] J. K. Furdyna, J. Appl. Phys. **64**, R29 (1988).
[4] S. Gopalan and M. G. Cottam, Phys. Rev. B **42**, 10311 (1990).
[5] C. Haas, Solid State Sci. **1**, 47 (1970).
[6] H. Ohno, Science **281**, 951 (1998).
[7] G. Medvedkin, T. Ishibaski, T. Niski, K. Hayata, Y. Hasagawa, and K. Sata, Jpn. J. Appl. Phys., Part 2 **39**, L949 (2000).
[8] G. A. Medvedkin, K. Hirose, T. Ishibashi, T. Nishi, V. G. Voevodin, and K. Sato, J. Cryst. Growth **236**, 609 (2002).
[9] S. Cho, S. Choi, G.-B. Cha, S. C. Hong, Y. Kim, Y.-J. Zhao, A. J. Freeman, J. B. Ketterson, B. J. Kim, Y. C. Kim, and B.-C. Choi, Phys. Rev. Lett. **88**, 257203 (2002).
[10] M. L. Reed, N. A. El-Masry, H. N. Stadelmaier, M. K. Ritums, M. J. Reed, C. A. Parker, J. C. Roberts, and S. M. Bekair, Appl. Phys. Lett. **79**, 3473 (2001).
[11] G. T. Thaler, M. E. Overberg, B. Gila, R. Frazier, C. R. Abernathy, S. J. Pearton, J. S. Lee, S. Y. Lee, Y. D. Park, Z. G. Kim, J. Kim, and F. Ren, Appl. Phys. Lett. **80**, 3964 (2002).
[12] N. Theodoropoulou, A. F. Hebard, M. E. Overberg, C. R. Abernathy, S. J. Pearton, S. N. G. Chu, and R. G. Wilson, Phys. Rev. Lett. **89**, 107203 (2002).
[13] S. A. Chambers, S. Thevuthasan, R. F. C. Farrow, R. F. Marks, J. U. Thiele, L. Folks, M. G. Samant, A. J. Kellock, N. Ruzycki, D. L. Ederer, and U. Diebold, Appl. Phys. Lett. **79**, 3467 (2001).
[14] Y. Matsumoto, M. Murakami, T. Shono, T. Hasegawa, T. Fukumaura, M. Kawasaki, P. Ahmet, T. Chikyow, S. Koshihara, and H. Koinuma, Science **291**, 854 (2001).
[15] S. Choi, G. B. Cha, S. C. Hong, S. Cho, Y. Kim, J. B. Ketterson, S. Y. Jeong, and G. C. Yi, Solid State Commun. **122**, 165 (2002).
[16] T. Dietl, H. Ohno, F. Matsukura, J. Cubert, and D. Ferrand, Science **287**, 1019 (2000).
[17] M. E. Overberg, C. R. Abernathy, S. J. Pearton, N. A. Theodoropoulou, K. T. McCarthy, and A. F. Hebard, Appl. Phys. Lett. **79**, 1312 (2001).
[18] T. Dietl, A. Haury, and Y. Merle d'Aubigne, Phys. Rev. B **55**, R3347 (1997).
[19] F. Holzberg, S. von Molnar, and J. M. D. Coey, in *Handbook on Semiconductors*, edited by T. S. Moss (North-Holland, Amsterdam, 1980), Vol. 3.
[20] B. E. Larson, K. C. Hass, H. Ehrenreich, and A. E. Carlsson, Solid State Commun. **56**, 347 (1985).
[21] K. Sato and H. Katayama-Yoshida, Jpn. J. Appl. Phys., Part 2 **39**, L555 (2000).
[22] T. Wakano, N. Fujimura, Y. Morinaga, N. Abe, A. Ashida, and T. Ito, Physica C **10**, 260 (2001).
[23] T. Fukumura, Z. Jin, A. Ohtomo, H. Koinuma, and M. Kawasaki, Appl. Phys. Lett. **75**, 3366 (1999).
[24] S. W. Jung, S.-J. An, G.-C. Yi, C. U. Jung, S.-I. Lee, and S. Cho, Appl. Phys. Lett. **80**, 4561 (2002).
[25] A. R. Hutson, Phys. Rev. **108**, 222 (1957).
[26] D. C. Look, J. W. Hemsky, and J. R. Sizelove, Phys. Rev. Lett. **82**, 2552 (1999).
[27] T. Story, Acta Physiol. Pol. **A91**, 173 (1997).